Charge calibration of MALTA2, a radiation hard depleted monolithic active pixel sensor

Lucian Fasselt[1,2*], Ignacio Asensi Tortajada[3], Prafulla Behera[4], Dumitru Vlad Berlea[1,2], Daniela Bortoletto[5], Craig Buttar[6], Valerio Dao[7], Ganapati Dash[4], Leyre Flores Sanz de Acedo[3], Martin Gazi[5], Laura Gonella[8], Vicente González[9], Sebastian Haberl[3], Tomohiro Inada[3], Pranati Jana[4], Long Li[10], Heinz Pernegger[3], Petra Riedler[3], Walter Snoeys[3], Carlos Solans Sánchez[3], Milou van Rijnbach[3], Marcos Vázquez Núñez[3,9], Anusree Vijay[4], Julian Weick[3], Steven Worm[1,2]

[1*]Deutsches Elektronen-Synchrotron DESY, Zeuthen, Germany.
[2]Humboldt University of Berlin, Berlin, Germany.
[3]CERN, Geneva, Switzerland.
[4]Indian Institute of Technology Madras, Chennai, India.
[5]University of Oxford, Oxford, UK.
[6]University of Glasgow, Glasgow, UK.
[7]Stony Brook University, New Yorck, US.
[8]Università degli Studi di Trieste, Trieste, Italy.
[9]Universitat de València, Valencia, Spain.
[10]University of Birmingham, Birmingham, UK.

*Corresponding author(s). E-mail(s): lucian.fasselt@desy.de;

Abstract

MALTA2 is a depleted monolithic active pixel sensor (DMAPS) designed for tracking at high rates and typically low detection threshold of $\sim \mathbf{150\,e^-}$. A precise knowledge of the threshold is crucial to understanding the charge collection in the pixel and specifying the environment for sensor application. A simple procedure is developed to calibrate the threshold to unit electrons making use of a dedicated charge injection circuit and an Fe-55 source with dominant charge deposition of $\mathbf{1600\,e^-}$. The injection voltage is determined which corresponds to the injection under Fe-55 exposure and is the basis for charge calibration. The charge injection circuit incorporates a capacitance with design value of $\mathbf{C_{inj}} = 230\,\mathrm{aF}$. Experimentally, the average capacitance value for non-irradiated samples is found to be $\mathbf{C_{inj,exp}} = 257\,\mathrm{aF}$. The 12 % divergence motivates the need for the presented precise calibration procedure, which is proposed to be performed for each MALTA2 sensor.

Keywords: DMAPS, Charge calibration, Tracking, High-energy physics

1 Introduction

MALTA2 is the second prototype of the MALTA family of depleted monolithic active pixel sensors (MAPS) designed in Tower 180 nm CMOS imaging sensor technology [1–3]. The MALTA2 pixel with a pitch of 36.4 µm consists of either high resistivity epitaxial or Czochralski silicon. The front-end in every pixel, as shown in figure 1, is optimized for threshold settings down to $\sim 150\,e^-$ for detection efficiencies above 99% as demonstrated for charged hadron beams [4]. The threshold is set globally by the different transistors, M0 to M9, by DAC settings corresponding to the gate of each transistor. Every pixel is also equipped with a dedicated charge injection circuit (figure 2). It makes use of two voltage settings V_{HIGH} and V_{LOW} and a V_{PULSE} signal. V_{HIGH} and V_{LOW} are subtracted by switching transistor M0 off and M1 on at the rising edge of V_{PULSE}. The resulting voltage difference is capacitively coupled to the input node of the front-end through a metal-to-metal connection that has a capacitance extracted from simulation of $C_{inj} = 230\,aF$ [5]. The injected charge is therefore:

$$Q_{inj} = C_{inj}\,\Delta V = C_{inj}(V_{HIGH} - V_{LOW}). \quad (1)$$

This document describes the procedure to measure the capacitance of the charge injection circuit of MALTA2 assuming a linear behaviour of the injected charge with respect to the difference of the V_{HIGH} and V_{LOW} voltages. ΔV_{Fe55} is the voltage difference that injects the same signal as an Fe-55 source. It is assumed that the charge deposited by the 5.9 keV K_α-line of an Fe-55 source is $1600\,e^-$. Radioactive sources with well defined X-ray lines are commonly selected for silicon sensors as calibration reference because of its point-like charge deposition. For thin sensors such as MALTA2, Fe-55 is selected due to its relatively low peak energy compared to other gamma sources and X-ray fluorescence lines [6, 7]. An alternative setup relying on Compton scattering requires multiple detectors as well as angle variation and is not suitable for frequent calibration of numerous samples [8]. In the following, the injected signals are quantified by the digital amplitude of the signal obtained through dedicated threshold scans, and ΔV_{Fe55} will be measured by dedicated source scans.

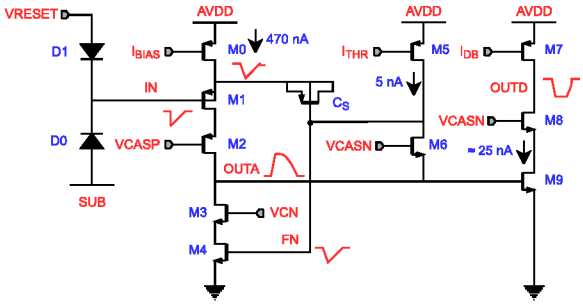

Fig. 1: MALTA2 front-end schematic including amplification, shaping and digitization of the analog signal per pixel [3]. IBIAS is the main biasing current and accounts for the majority of the power consumption. The current ITHR defines the speed of the feedback loop and is designed to linearly effect the threshold of the discriminator.

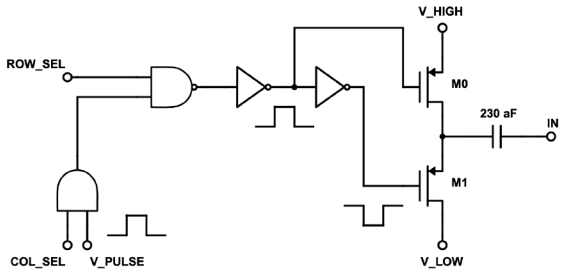

Fig. 2: MALTA2 charge injection circuit [5].

2 Methods

2.1 Voltage measurement

The voltages V_{HIGH} and V_{LOW} are controlled by a DAC with a 7-bit range. The voltage produced by the DAC as a function of the value of V_{HIGH} as measured with a Keithley 2400 is shown in figure 3. A linear regime is observed from DAC value 0 to 90 with a gradient of 13.5 mV/DAC and an offset of 0.45 V. This value will be used to calculate the expected voltage of V_{HIGH}. The behaviour of the V_{LOW} DAC is identical. For DAC values larger than 90 the voltage saturates due to a buffer stage which adds a voltage shift of 0.4 V and restricts the linear voltage generation.

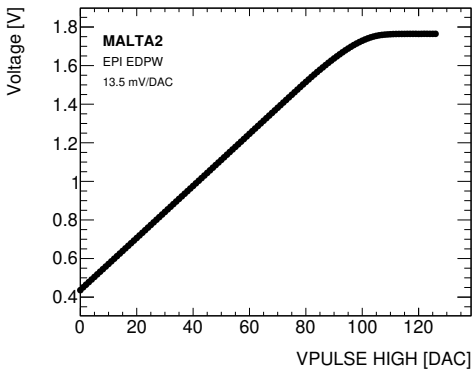

Fig. 3: V_{HIGH} voltage characteristic curve generated at the respective DAC value. The linear responds with a gradient of 13.5 mV/DAC holds up to a DAC value of 90.

2.2 Digital amplitude of injected charge

A threshold scan is a variation of the ITHR current DAC that is proportional to the threshold set in the discriminator in the pixel front-end. It is proportional to the speed at which the signal returns to the baseline. From the binary hit data, a signal can be quantified in a threshold scan through the digital amplitude, that is the threshold at which the number of hits are reduced to 50%. Figure 4a parameterises the digital amplitude of charge injected into a single pixel through an s-curve

$$s(x; C, a, b) = \frac{C}{2}\left[1 - \mathrm{erf}\left(\frac{x-a}{\sqrt{2}b}\right)\right] \qquad (2)$$

with the error-function definition

$$\mathrm{erf}\,(z) = \frac{2}{\sqrt{\pi}}\int_0^z \mathrm{e}^{-t^2}dt. \qquad (3)$$

Its differentiation

$$\frac{d}{dx}s(x; C, a, b) = -C\,\mathcal{N}\left(a, b^2\right) \qquad (4)$$

results in a Gaussian distribution with prefactor C, mean a and standard deviation b. The digital amplitude is quantified through the position parameter a of the error-function. The histogram of the digital amplitudes for all pixels in figure 4b is described by a Gaussian distribution with mean amplitude $\mu = 40.0$ and standard deviation $\sigma = 5.3$ that quantifies pixel-to-pixel variations.

According to equation 1, the injected charge ideally depends on $\Delta V = V_{HIGH} - V_{LOW}$ but not on the individual setting of the two DAC values. Consequently, a variation of V_{HIGH} and V_{LOW} should not affect the digital amplitude when keeping ΔV constant. Figure 5 shows the mean digital amplitude as a function of V_{HIGH} and V_{LOW} while keeping ΔV constant at 10, 15, 20 and 25. A plateau forms for all ΔV which defines the range in which all injections yield the same amplitude. At this plateau the amplitude does not depend on the specific value of V_{HIGH} or V_{LOW}. The plateau is restricted towards large DAC values by $V_{HIGH} \leq 90$ and towards small DAC values by $V_{LOW} \geq 20$. Both restrictions are indicated by dashed lines. At low voltages the PMOS transistors that do switching between V_{HIGH} and V_{LOW} saturate. Hence, a reliable injection is obtained when keeping the DAC values within the range [20,90]. From this follows a maximum injection at $\Delta V = 70$.

2.3 Digital amplitude of Fe-55 source

A gamma source of Fe-55 is used commonly as a calibration source for thin silicon sensors because the charge deposition through photon absorption is around 1600 e^- which corresponds to the most probable charge deposition of a minimum-ionizing particle in 27 µm of silicon [9]. The source emits photons at the K_α-lines of 5.9 keV. The MALTA2 front-end is designed for thresholds down to $\sim$ 150 e^- to ensure high detection efficiency of minimum-ionizing particles [3]. As a result, the usual threshold range is far below the charge deposition of 1600 e^-. However, a low bias current setting in the front-end allows to suppress the gain and configure the threshold to values $> 2000\,e^-$. In such a low-gain setting, a threshold scan is sensitive to the amplitude deposited by soft X-rays. A threshold scan of all pixels of a MALTA2 sensor under exposure of an Fe-55 source is shown in figure 6. An error-function fit describes the decrease in hits towards large thresholds and yields a digital amplitude of $a_{Fe55} = 62$. The width parameter $b_{Fe55} = 11$ incorporates pixel-to-pixel variations.

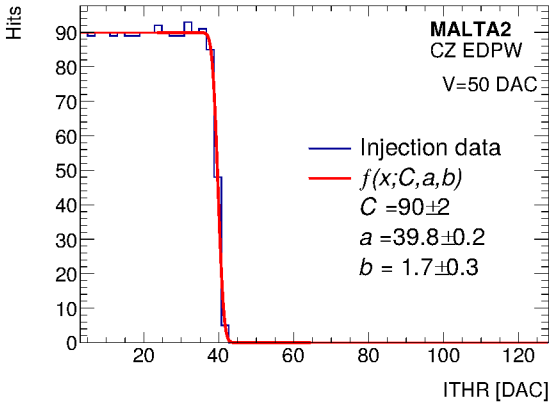

(a) Threshold scan of a single pixel under charge injection.

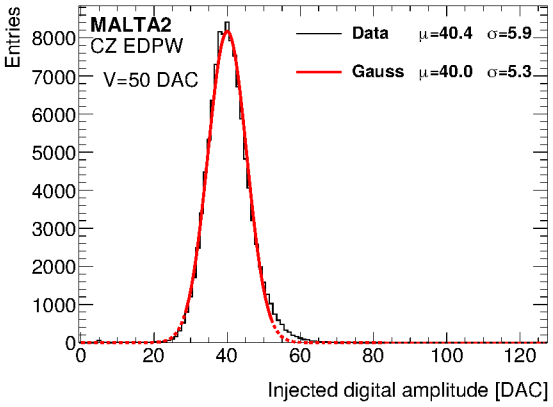

(b) Histogram of digital amplitudes for all pixels.

Fig. 4: The digital amplitude from charge injection with $\Delta V = V_{HIGH} - V_{LOW} = 50$ DAC is obtained in (a) for a single pixel through the position parameter a of an error-function fit with width b. The factor C scales with the number of injected pulses. As the threshold DAC current ITHR is raised above the injected signal the number of detected hits decreases. The histogram in (b) of digital amplitudes for all 224×512 pixels is described by a Gaussian fit to the core of the distribution. The stated values of the mean μ and the standard deviation σ are those calculated from the data or obtained through the fit.

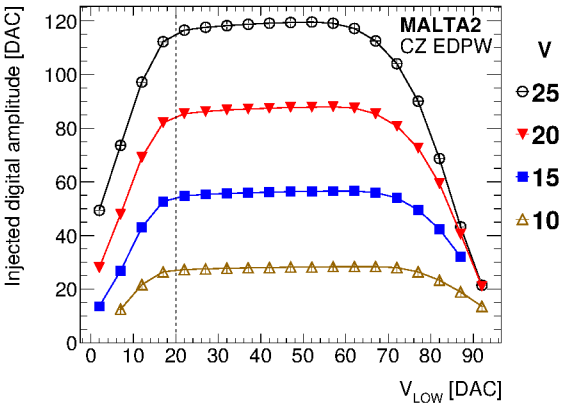

(a) Injected digital amplitude versus V_{LOW}.

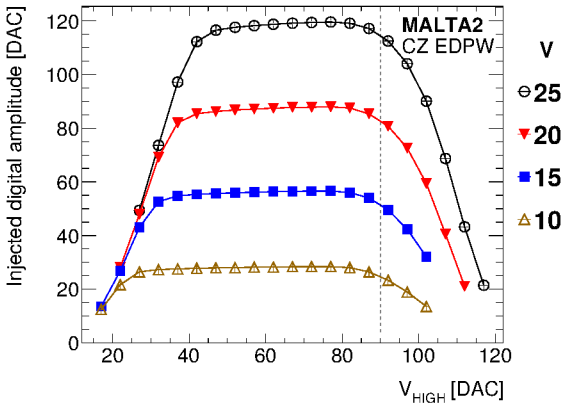

(b) Injected digital amplitude versus V_{HIGH}.

Fig. 5: Injected digital amplitude versus V_{LOW} and V_{HIGH}. The digital amplitude remains constant in a stable DAC range of [20,90]. The dashed lines mark the lower boundary for V_{LOW} and the upper boundary for V_{HIGH}. Outside that range, saturation effects reduce the injected charge which in turn causes a reduction in digital amplitude.

3 Calibration Results

3.1 Charge calibration through Fe-55 source

Charge is injected for different values of ΔV and the mean digital amplitude is reconstructed

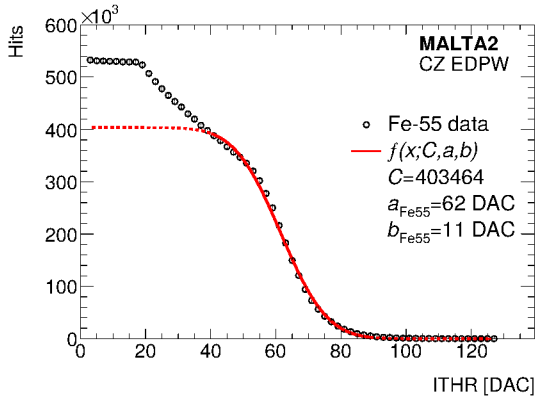

Fig. 6: Threshold scan under exposure of an Fe-55 source. Data points (black dots) are the sum of hits from a MALTA2 sensor. The error-function fit (red line) is fitted to the high threshold regime (solid line) to parameterise the absorption of K_α photons of 5.9 keV. The function is continued outside the fit regime (dashed line). The parameter a_{Fe55} marks the position of the falling edge and b_{Fe55} the width describing pixel-to-pixel variations. The deviation of fit function and data at low thresholds is due to charge sharing where an absorbed photon near a pixel corner causes multiple hits.

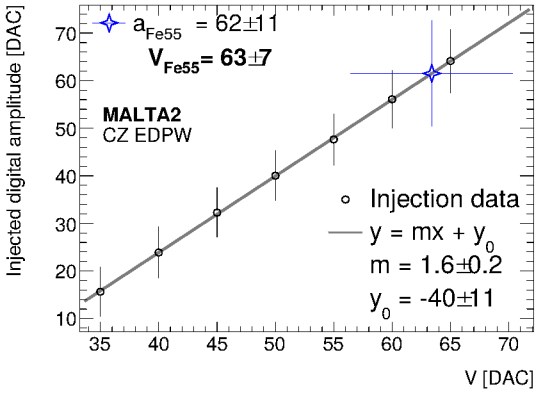

Fig. 7: Average digital amplitude versus injection DAC setting. Data points represent the mean from the Gaussian fit to all pixel amplitudes and the error bars represent the standard deviation. The digital amplitude a_{Fe55} from the Fe-55 detection is added as a calibration point to interpolate from the linear fit the corresponding charge injection ΔV_{Fe55} that yields the same digital amplitude.

according to the example for $\Delta V = 50$ in figure 4. The amplitude is found to be proportional to ΔV as shown in figure 7. The independently measured digital amplitude a_{Fe55} under the exposure of the Fe-55 source is used as a charge calibration point. From the linear fit the corresponding ΔV_{Fe55} value is calculated. The charge injected through the circuit at ΔV_{Fe55} yields the same amplitude as a_{Fe55}.

Further, the injection capacitance is calculated as

$$C_{inj} = \frac{1600\,e^- \times 1.602 \times 10^{-19}\,C/e^-}{\Delta V_{Fe55} \times 13.5\,mV/DAC} = \frac{19\,000\,aF}{\Delta V_{Fe55}/DAC} \quad (5)$$

by assuming a voltage input per unit ΔV in the injection circuit of 13.5 mV/DAC.

Table 1 lists the calibration results of ΔV_{Fe55} and C_{inj} for all tested samples. Considering only the six non irradiated samples an average injection capacitance of

$$C_{inj,exp} = 257\,aF \quad (6)$$

is found to be 12% larger than the design value of $C_{inj} = 230\,aF$. For the Fe-55 equivalent injection DAC the average value is determined to be

$$\Delta V_{Fe55,exp} = 75 \pm 10\,DAC. \quad (7)$$

The stated uncertainty is the standard deviation of the sample and estimates the fluctuation among different sensors originating from the fabrication process.

3.2 Calibrated threshold scans

Based on the result of ΔV_{Fe55} any charge injected into a MALTA2 sensor can be calibrated to unit electrons according to

$$Q_{inj} = \Delta V \frac{1600\,e^-}{\Delta V_{Fe55}}. \quad (8)$$

For a normal and low gain front-end setting the detection threshold is measured as an average over all pixels and is shown in figure 8. The low gain is the result of reducing the main front-end bias current IBIAS by a factor of 14 compared

Table 1: MALTA2 Calibration Results

sample	doping	NIEL $[10^{15}\,n_{eq}cm^{-2}]$	ΔV_{Fe55} [DAC]	C_{inj} [aF]
W5R21	high	0	76 ± 7	250 ± 23
W8R24	low	0	87 ± 9	218 ± 23
W11R0	high	0	63 ± 7	301 ± 33
W14R11	high	0	85 ± 8	223 ± 21
W18R17	very high	0	75 ± 6	253 ± 20
W18R19	very high	0	64 ± 5	297 ± 23
W12R7	high	1	66 ± 8	288 ± 35
W18R1	very high	1	65 ± 8	292 ± 36
W18R4	very high	2	58 ± 8	327 ± 45
W18R9	very high	3	47 ± 6	404 ± 52
W18R21	very high	3	53 ± 6	358 ± 41
W18R12	very high	5	46 ± 10	413 ± 90
W18R14	very high	5	41 ± 8	463 ± 90

to the normal setting and leads to larger threshold values. The thresholds in unit electrons (left y-axes) are obtained through equation 8 based on the measurement of ΔV (right y-axes). Error bars quantify the error on the mean threshold and are of the same order than the marker size. The threshold dependence on ITHR can be parameterised by a linear or quadratic function. These threshold values define the detection threshold at testbeam studies and beam telescope applications [4, 10]. The threshold resolution quantifying the standard deviation from pixel to pixel variations is around 10%.

3.3 Irradiation study

A selection of samples from the same wafer of 100 µm thick Czochralski silicon with very high doping of the n- layer has been neutron irradiated at different fluences of non-ionizing energy loss (NIEL) at the Triga reactor in the Institute Jožef Stefan (IJS), Slovenia. The calibration results are compared in figure 9 and show a decrease in the Fe-55 equivalent injection voltage ΔV_{Fe55} with fluence. In irradiated samples, a lower injection voltage is needed to inject 1600 e^-. This can be interpreted as an increase in the apparent injection capacitance. Two sensors are tested for each of the fluences at 1, 3 and $5 \times 10^{15}\,n_{eq}cm^{-2}$ and show compatibility within the order of the stated uncertainties. The study shows that charge calibration has to account for the irradiation fluence for precise threshold determination.

4 Summary

The charge injection circuit of MALTA2 sensors has been calibrated inside a reliable DAC range of [20,90] for the parameters V_{HIGH} and V_{LOW}. A digital amplitude is reconstructed through threshold scans from binary hit data as the position parameter of an error-function fit. The amplitude is proportional to the voltage input of the charge injection circuit $\Delta V = V_{HIGH} - V_{LOW}$ and is calibrated through an Fe-55 source. Based on this, the charge injected into a MALTA2 sensor can be calculated:

$$Q_{inj} = \Delta V \frac{1600\,e^-}{\Delta V_{Fe55}} \tag{9}$$

It is proposed that for precise calibration ΔV_{Fe55} is determined for each sample. For the six tested non irradiated sensors the mean and standard deviation of $\Delta V_{Fe55,exp} = 75 \pm 10$ is obtained. The mean value is assumed for calibration of non irradiated samples that are not calibrated individually. Neutron irradiated samples show a smaller value of V_{Fe55} due to an increase in the effective injection capacitance. Once the charge calibration parameter ΔV_{Fe55} is obtained, the threshold setting of a MALTA2 sensor is quantifiable at

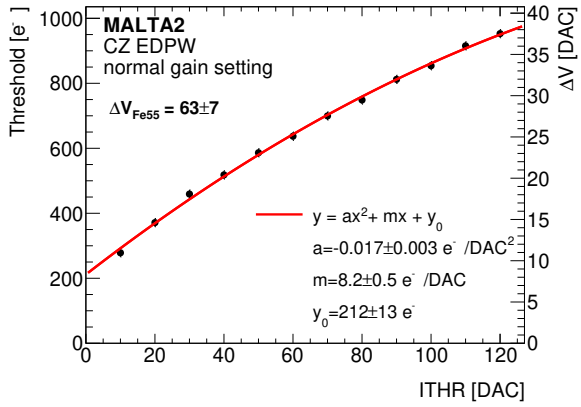

(a) Thresholds for front-end at normal gain.

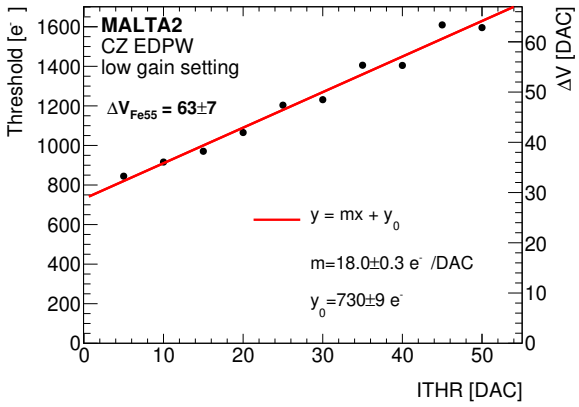

(b) Thresholds for front-end at low gain.

Fig. 8: Calibrated threshold as a function of the ITHR DAC. For each ITHR value, the threshold is measured per pixel in units of injected charge ΔV (right y-axes). The calibration input of ΔV_{Fe55} makes a linear calibration to unit electrons according to equation 8 possible (left y-axes). (a) shows a normal gain setting at IBIAS=43 with thresholds down to 200 e^- and a parabolic fit. (b) shows a low gain front-end setting at IBIAS=3 with thresholds above 750 e^- and a linear fit.

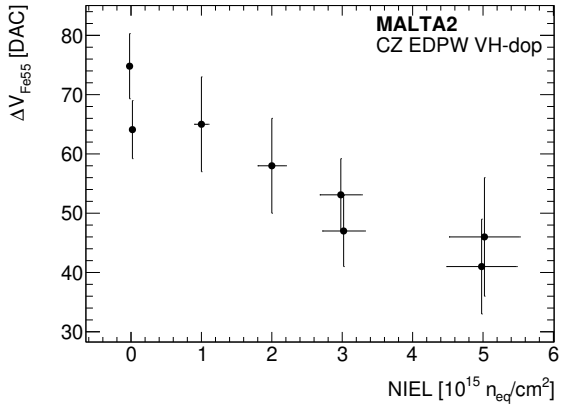

(a) ΔV_{Fe55} versus NIEL.

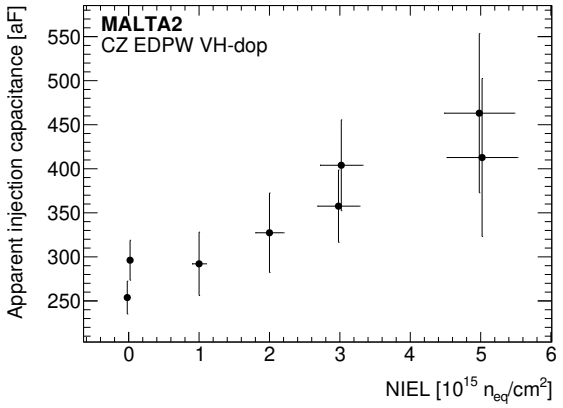

(b) Apparent injection capacitance versus NIEL.

Fig. 9: Dependence of ΔV_{Fe55} (a) and the corresponding injection capacitance (b) on the irradiation fluence as non-ionizing energy loss (NIEL). All samples originate from the same wafer of 100 µm thick Czochralski silicon with very high doping of n- layer. ΔV_{Fe55} is the voltage DAC value that injects a charge of 1600 e^- corresponding to the main Fe-55 deposition. ΔV_{Fe55} decreases with irradiation. Consequently, the apparent injection capacitance increases with irradiation because a lower voltage is needed to inject the same reference charge.

any front-end setting through charge injection. The described procedure is feasible for any binary sensor that incorporates an injection circuit.

Acknowledgements. This project has received funding from the European Union's Horizon 2020 Research and Innovation programme under

Grant Agreement number 101004761 (AIDAinnova), and number 654168 (IJS, Ljubljana, Slovenia). Furthermore it has been supported by the Marie Sklodowska-Curie Innovative Training Network of the European Commission Horizon 2020 Programme under contract number 675587 (STREAM). This publication was funded by Deutsche Forschungsgemeinschaft (DFG, German Research Foundation) - 491245950.

References

[1] Pernegger, H., *et al.*: First tests of a novel radiation hard CMOS sensor process for Depleted Monolithic Active Pixel Sensors. JINST **12**(06), 06008 (2017) https://doi.org/10.1088/1748-0221/12/06/P06008

[2] Berdalovic, I., *et al.*: MALTA: a CMOS pixel sensor with asynchronous readout for the ATLAS High-Luminosity upgrade. In: Proc. IEEE Nucl. Sci. Symp. Med. Imag. Conf., p. 8824349 (2018). https://doi.org/10.1109/NSSMIC.2018.8824349

[3] Piro, F., et al.: A 1 μW radiation-hard front-end in a 0.18 μm CMOS process for the MALTA2 monolithic sensor. IEEE Trans. Nucl. Sci. **69**(6) (2022) https://doi.org/10.1109/TNS.2022.3170729

[4] van Rijnbach, M., *et al.*: Radiation hardness of MALTA2 monolithic CMOS imaging sensors on Czochralski substrates. Eur. Phys. J. C **84**(3), 251 (2024) https://doi.org/10.1140/epjc/s10052-024-12601-3 arXiv:2308.13231

[5] Berdalovic, I.: Design of radiation-hard CMOS sensors for particle detection applications. PhD thesis, Zagreb U. (2019). Presented 29 Oct 2019. http://cds.cern.ch/record/2702884

[6] Pohl, D.-L., *et al.*: Obtaining spectroscopic information with the ATLAS FE-I4 pixel readout chip. NIMA **788**, 49–53 (2015) https://doi.org/10.1016/j.nima.2015.03.067

[7] Fasselt, L., et al.: Energy calibration through X-ray absorption of the DECAL sensor, a monolithic active pixel sensor prototype for digital electromagnetic calorimetry and tracking. Frontiers in Physics **11** (2023) https://doi.org/10.3389/fphy.2023.1231336

[8] McCormack, P., et al.: New Method for Silicon Sensor Charge Calibration Using Compton Scattering (2020). https://arxiv.org/abs/2008.11860

[9] Meroli, S., *et al.*: Energy loss measurement for charged particles in very thin silicon layers. JINST **6**(06), 06013 (2011) https://doi.org/10.1088/1748-0221/6/06/P06013

[10] Gustavino, G., *et al.*: Development of the radiation-hard MALTA CMOS sensor for tracking applications. In: Proc. Vertex 2023, vol. 448, p. 048 (2024). https://doi.org/10.22323/1.448.0048

Appendix A Calibrated samples

Figures A1-A5 show the calibration results for all 13 calibrated sensors of which six are not irradiated. They correspond to the Fe-55 threshold scan and injection calibration as described for the example sensor in figs. 6, 7. All calibration results are summarized in table 1.

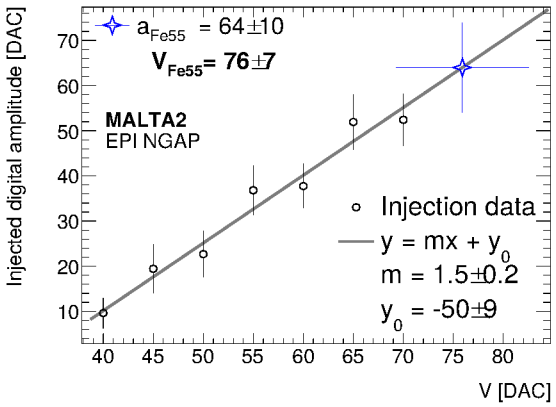

(a) W5R21

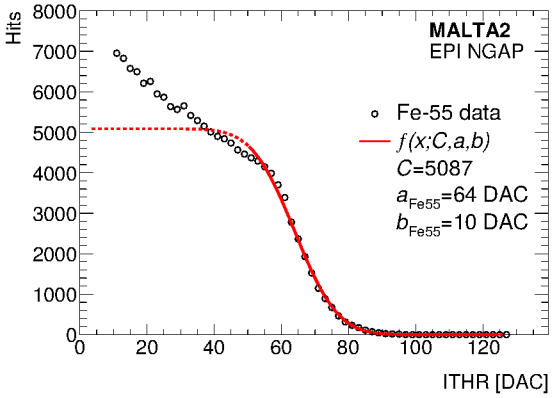

(b) W5R21

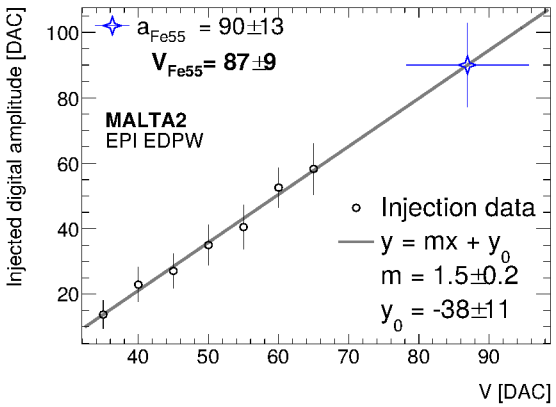

(c) W8R24

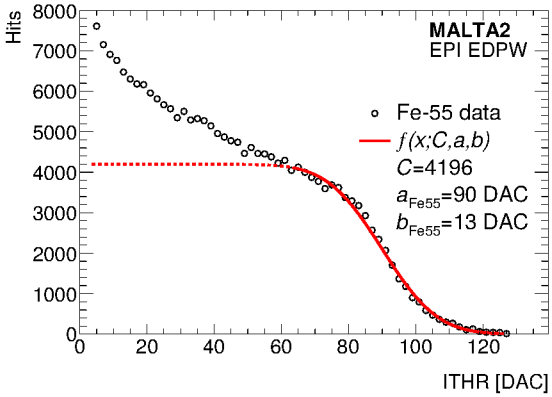

(d) W8R24

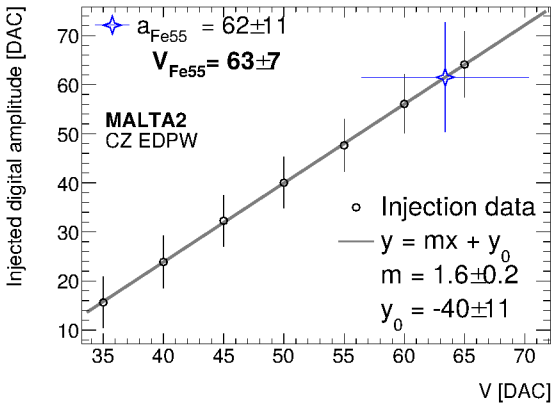

(e) W11R0

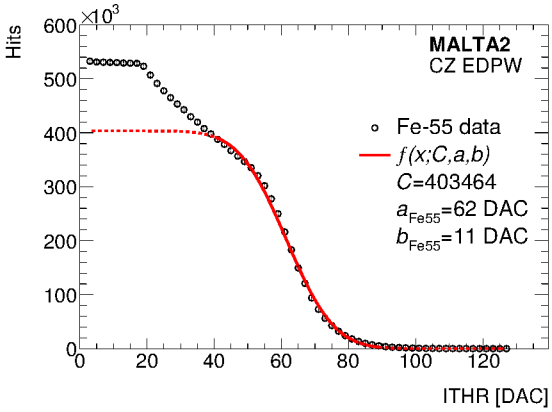

(f) W11R0

Fig. A1

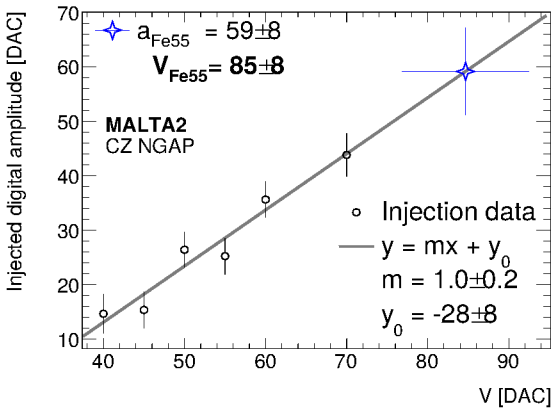

(a) W14R11

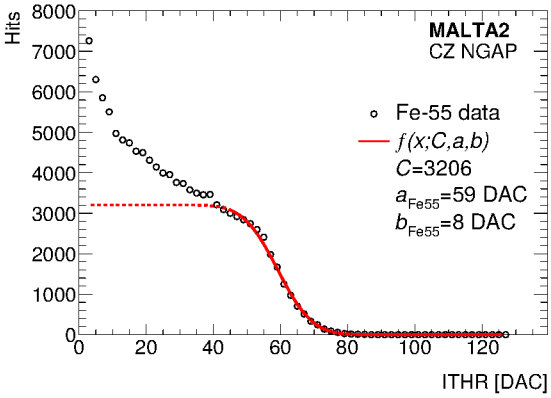

(b) W14R11

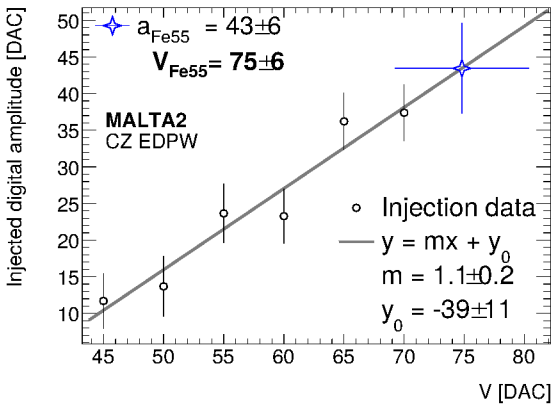

(c) W18R17

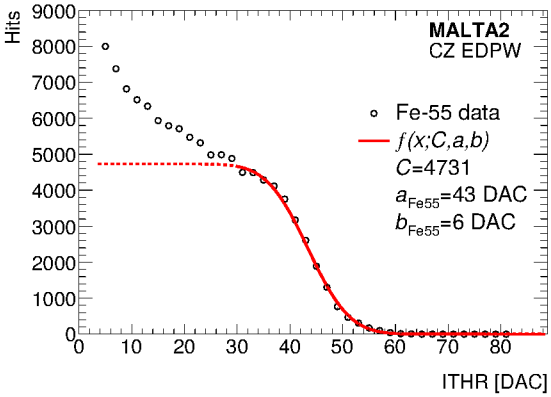

(d) W18R17

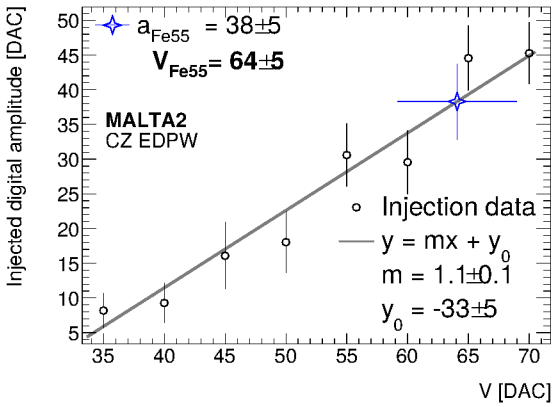

(e) W18R19

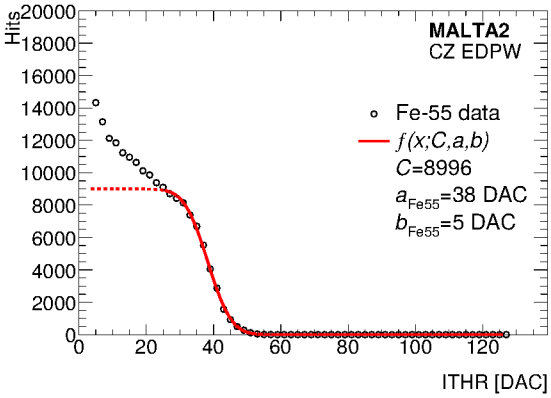

(f) W18R19

Fig. A2

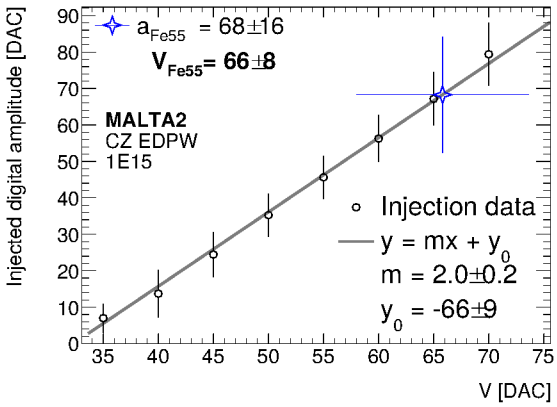

(a) W12R7 (1E15)

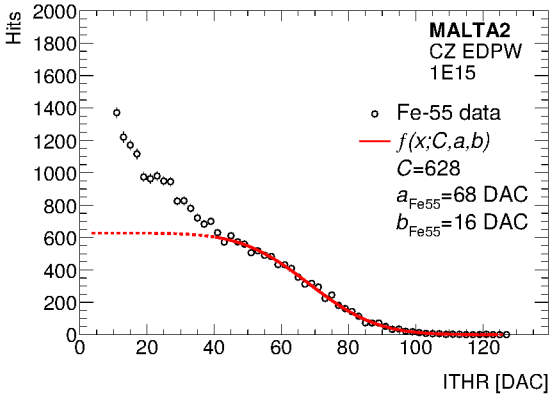

(b) W12R7 (1E15)

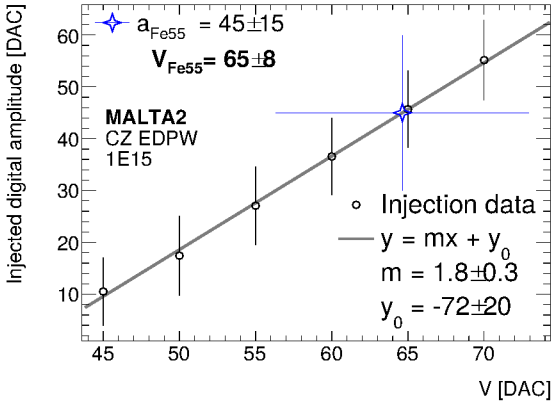

(c) W18R1 (1E15)

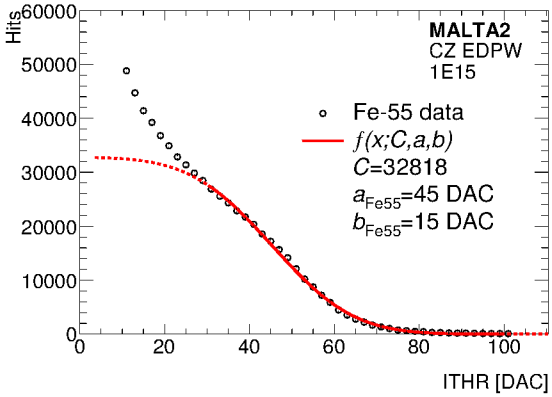

(d) W18R1 (1E15)

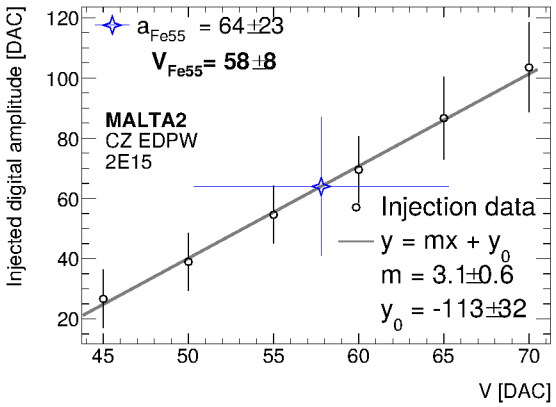

(e) W18R4 (2E15)

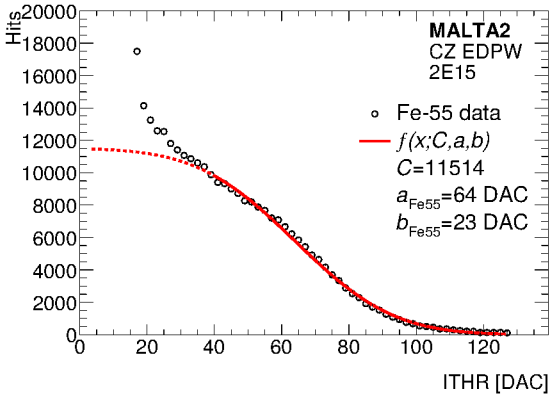

(f) W18R4 (2E15)

Fig. A3

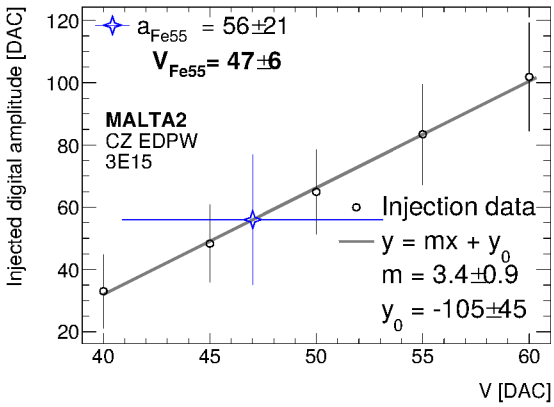

(a) W18R9 (3E15)

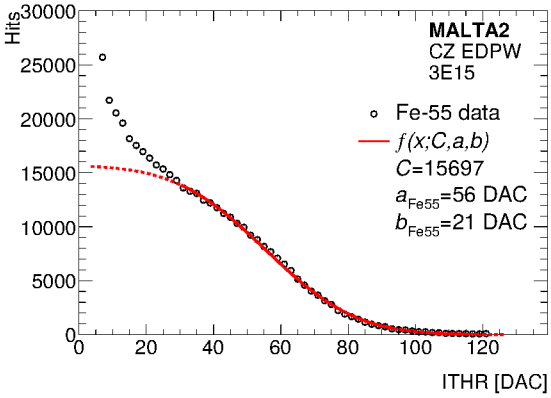

(b) W18R9 (3E15)

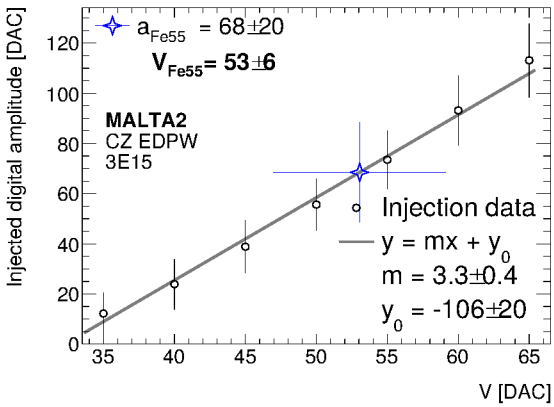

(c) W18R21 (3E15)

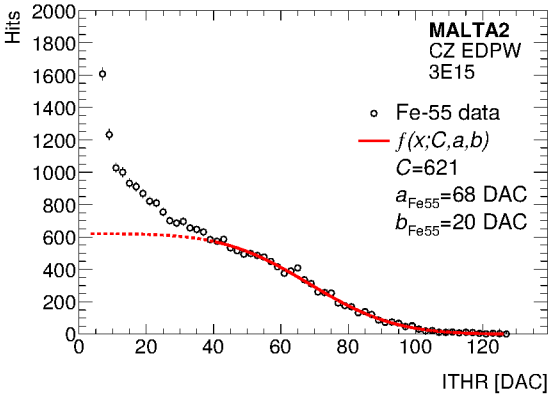

(d) W18R21 (3E15)

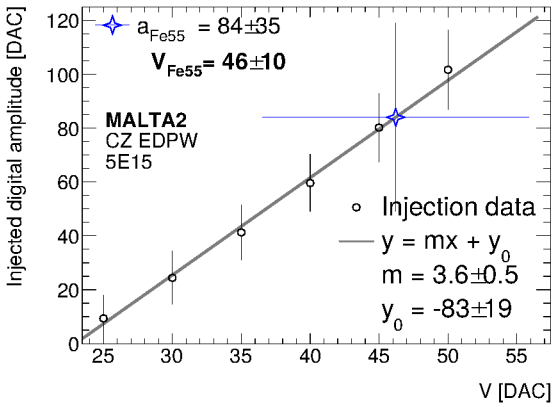

(e) W18R12 (5E15)

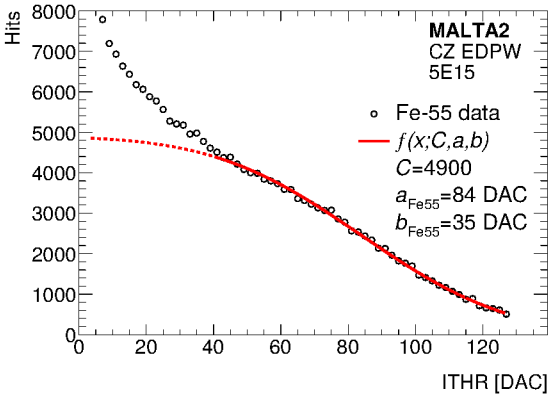

(f) W18R12 (5E15)

Fig. A4

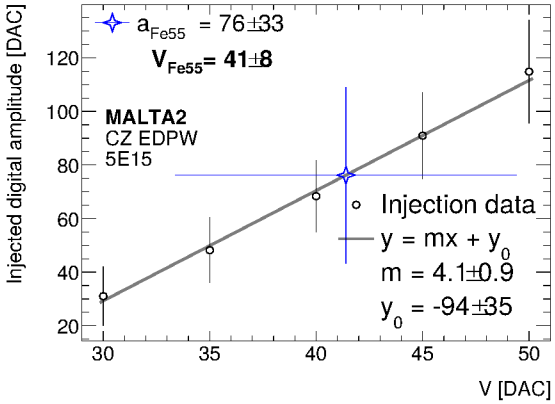

(a) W18R14 (5E15)

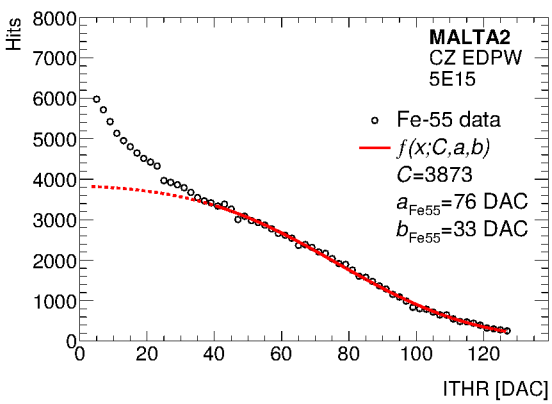

(b) W18R14 (5E15)

Fig. A5